Self-consistent field theory of protein adsorption in a non-Gaussian polyelectrolyte brush

P. Maarten Biesheuvel,* Frans A. M. Leermakers, and Martien A. Cohen Stuart
Laboratory of Physical Chemistry and Colloid Science, Wageningen University, Dreijenplein 6, 6703 HB Wageningen, The Netherlands
(Received 6 October 2005; published 30 January 2006)

To describe adsorption of globular protein molecules in a polyelectrolyte brush we use the strong-stretching approximation of the Edwards self-consistent field equation, combined with corrections for a non-Gaussian brush. To describe chemical potentials in this mixture of (globular) species of widely varying sizes (ions, brush polyelectrolyte segments, globular protein molecules), we use the Boublik-Mansoori-Carnahan-Starling-Leland equation of state derived for polydisperse mixtures of spherical particles. The polyelectrolyte chain is described in this approach as a string of beads with the beads of a size related to the chain diameter. We use the one-dimensional Poisson equation to describe the electrostatic field and include the ionizable character of both the brush polyions and the protein molecules. This model explains the experimental observation of high amounts of protein adsorption in a polyacid brush for *p*H values above the isoelectric point of the protein as being due to charge reversal of the protein molecules upon entry in the brush. We find a distinct minimum in protein concentration near the edge of the brush. With increasing *p*H this barrier to protein transfer becomes larger, but much less so when we increase the ionic strength, a difference that might relate to an experimentally observed difference in the protein release rate in these two cases. A free energy analysis shows that the release of small ions from the brush and the increase of brush ionization are the two driving forces for protein adsorption in a like-charged brush.

DOI: 10.1103/PhysRevE.73.011802 PACS number(s): 36.20.−r, 82.35.Rs, 87.14.Ee, 87.15.Kg

I. INTRODUCTION

The globular protein bovine serum albumin (BSA) adsorbs in significant quantities in carboxylic acid brushes grafted on ~100-nm-sized nanoparticles (so-called "spherical brush particles"), even for *p*H values above the isoelectric point of the protein, when both protein and polyion are negatively charged [1–4]. This phenomenon occurs mainly for a *p*H still close to *p*I and for a sufficiently low ionic strength.

To describe these experimental findings theoretically, we recently constructed a spherical box model for annealed polyelectrolyte that includes adsorption of protein molecules [5]. In such a box model local charge electroneutrality is assumed, while all free ends are located at the edge of the brush. Modifications compared to traditional brush box models were the inclusion of the volume of brush polyions and protein molecules in the local electroneutrality balance (effectively excluding small ions and resulting in an increase of the chemical potential of the polyions and protein), as well as the finite, non-Gaussian, stretching of the polyelectrolyte chains, incorporated using an overstretching term. Volume interactions between the polyions were included using Flory-Huggins theory, while for protein molecules such interactions were described using the Carnahan-Starling equation of state. However, volume interactions between brush segments and protein molecules were neglected. In the charge balance the ionizable character of both the brush and protein molecules was included (namely, that the charge depends on the local proton concentration), while a related chemical term was added to the chemical potential. Nonelectrostatic (energetic) interactions (hydrophobic, van der Waals, etc.) between the different species were neglected.

Despite these simplifications, the box model could qualitatively describe data for the influence of *p*H and ionic strength on the adsorbed amount of protein in the brush, most strikingly the fact that protein is able to adsorb at a *p*H above its own isoelectric point *p*I, where it is of the same charge sign as the brush. The explanation of this phenomenon is the charge reversal of the protein molecules upon entering the brush, which, in agreement with the data, is only possible at a *p*H not too much above the isoelectric point (for BSA, *p*I=5.1) and at sufficiently low ionic strength. It must be noted, however, that the model is oversensitive to the influence of *p*H and ionic strength: whereas in reality adsorption already starts at *p*H 7 and gradually increases with decreasing *p*H [1], in the model a sharp transition is predicted in a 0.1 *p*H window around *p*H 5.6. A similar sharp transition, not observed, is predicted for the ionic strength.

To improve on the earlier approach we combine several elements into a more accurate brush model. First of all, instead of making the "box" assumption that all chains have their free ends at the same distance from the surface, we will use the strong-stretching limit of the self-consistent field (Edwards) equation [6–17] and use the corrections required for a non-Gaussian brush given by Amoskov and Pryamitsyn [16,17] for finite stretching. Instead of assuming local charge neutrality, the full Poisson equation is used both inside and outside the brush. To describe volume interactions between brush segments, ions, and protein molecules self-consistently, we use an excess function based on work by Boublik [18] and Mansoori, Carnahan, Starling, and Leland [19] (BMCSL) who extend the Carnahan-Starling equation of state to multicomponent mixtures of (spherical) particles of unequal size. The BMCSL function self-consistently describes all volume interactions, between like and unlike spe-

*Electronic address: maarten.biesheuvel@wur.nl

cies alike (brush segments, protein molecules, and the two types of small ions). When the different species in the system have widely different sizes, this may be a very useful and elegant approach; incorporating these effects in the (lattice-based) Flory-Huggins formalism is more difficult. It must be noted that in this approach the correlations between chain segments because of their connectness are neglected; instead, the same (mean-field) assumption is made as in Flory-Huggins theory. The use of the BMCSL function has similarities with some elements from the hard-sphere self-associating fluid theory (HS-SAFT) for polymer solutions (see, e.g., Ref. [20]), while Misra and Varanasi [14] use a similar approach to describe the excess contribution to the chemical potential of ions. However, the brush segment potential is not influenced by the volume of ions in their approach.

Related theoretical work is by Simmons *et al.* [21] who described the adsorption of polyelectrolyte in the corona of an oppositely charged diblock copolymer micelle and by Moskovitz and Srebnik [22] who use a two-dimensional self-consistent-field model to describe protein adsorption in a polymer brush, but do not include electrostatic effects (see also their Refs. [31–40]). A mean-field theory for protein adsorption in a brush is presented in Ref. [23], leaving out electrostatic effects. Some other theoretical work is summarized in Ref. [5].

Sections II and III are based on analyzing the potentials of brush segments and protein molecules which at equilibrium are independent of location. This analysis results in equilibrium brush density profiles and protein-adsorbed amounts; however, it does not give quantitative information on the magnitude of the different energies involved during protein adsorption. Such a free energy analysis is presented in the Appendix.

Note that we will use the terms "polyion," "brush," and "polyelectrolyte" alternatingly to describe the flexible, grafted, chains. The globular protein molecule that adsorbs in the brush is assumed to be a rigid (spherical) particle.

II. THEORY

A. Non-Gaussian brush

For a monodisperse brush (all chains of the same length) and in the strong-stretching limit the Edwards self-consistent field equation predicts a parabolic dependence of the conformational (stretching, elasticity, etc.) contribution to the potential μ as a function of the distance from the grafting interface, x [6–17]. The potential (of a brush segment, an ion, a protein molecule, etc.) is defined here to contain all possible contributions (including, for the brush, stretching) and at equilibrium is constant across the brush. The conformational contribution μ^{conf} increases with x according to

$$\mu^{conf} = \mu_0 + \frac{3\pi^2}{8k}\left(\frac{x}{L}\right)^2, \tag{1}$$

where L is the contour length and k the Kuhn length. Note that throughout this paper all potentials are scaled with the thermal energy kT. Because for a polyelectrolyte brush with a high line charge density (relative to the Kuhn length) a brush extension beyond the contour length is readily predicted when we use Eq. (1) (especially at low ionic strength [14]), we will use the higher-order corrections to the parabolic, Gaussian, brush given by Amoskov and Pryamitsyn [16,17]—namely,

$$\mu^{conf} = \mu_0 + \frac{1}{k}\sum_i V_i\left(\frac{x}{L}\right)^{2i}, \tag{2}$$

with V_i the prefactors given for the freely jointed chain in Ref. [16], Table 1 (starting with $V_1 = 3\pi^2/8 \sim 3.7011$; note that only even powers are required in the summation). The polyelectrolyte brush theory by Misra and Varanasi [14] uses a different finite-extensibility correction [12], one that according to Amoskov and Pryamitsyn [16] is incorrect.

B. Electrostatics

The Poisson equation relates the mean-field electrostatic potential ψ to the local charge density ρ according to

$$\varepsilon_0 \nabla (\varepsilon_{eff} \nabla \psi) = -\rho, \tag{3}$$

where the electrostatic potential ψ relates to the dimensionless variable y as $y = e\psi/kT$ while ρ incorporates the local concentrations c_i of the various charged species (ions, brush segments, protein molecules) and their charge Z_i.

In Eq. (3) we have included the fact that the local permittivity ε_{eff} may depend on position. This permittivity correction has an effect on the Poisson equation and results as well in a polarization contribution to the potential of the different species [24–26]. In the current calculation, however, the influence of the permittivity effect is very small because the brush is either close to charge neutral (interior of the brush, low $\nabla\psi$) or very dilute (outer edge, low $\nabla\varepsilon_{eff}$). Therefore, to keep the exercise as simple as possible we will assume a constant permittivity throughout (namely, that of water, ε_w), after which Eq. (3) results for a one-dimensional, spherical, geometry in

$$\frac{\partial^2 y}{\partial r^2} + \frac{2}{r}\frac{\partial y}{\partial r} = -\kappa^2 \sum_j \frac{Z_j c_j}{2c_\infty}, \tag{4}$$

where the summation contains protein molecules, brush segments, and ions and where the Debye length κ^{-1} is defined as

$$\kappa^2 = \frac{2c_\infty e^2}{\varepsilon_0 \varepsilon_w kT}, \tag{5}$$

with c_∞ the ionic strength defined in a protein-free reservoir phase (where we will also define pH). When we describe the ions as point charges and thus neglect their volume, Eq. (4) simplifies to

$$\frac{\partial^2 y}{\partial r^2} + \frac{2}{r}\frac{\partial y}{\partial r} = \kappa^2\left((1-\phi)\sinh y - \sum_j \frac{Z_j c_j}{2c_\infty}\right), \tag{6}$$

where the summation now only contains the brush segments and the protein molecules, and ϕ is their summed volume fraction. The factor "$1-\phi$" is due to a correction to the chemical potential of the pointlike ions due to the volume of

protein and brush segments, and can be rigorously derived from the BMCSL formalism for the equation of state of a multicomponent mixture of hard spheres [18,19] as we show in Ref. [26]. This approach is also in exact agreement with the way Biben and Hansen [27] deal with the small ions in the context of sedimenting charged colloids.

C. Charge regulation

For ionizable polyions and protein, the charge Z_i depends on the local proton concentration and thus on the electrostatic potential y. Note that we only consider proton adsorption and desorption, and neglect adsorption of other ions, while we will closely follow earlier literature on this subject [5,15,24,25,28–30]. Briefly, the ionization degree of a monomeric group (e.g., carboxylic acid monomer, or amino acid residue) is given by

$$\alpha = \frac{1}{1 + 10^{z(p\mathrm{H}-p\mathrm{K})}e^{zy}}, \tag{7}$$

where pK is the *intrinsic* pK value, a thermodynamic number dependent on the proton adsorption energy. pK values are tabulated and must not be confused with *apparent* pK values which are a measure of the ionization degree α. pH is defined in the protein- and brush-free reservoir where we set $y=0$; z describes whether the ionizable group is cationic ($z=1$) or anionic ($z=-1$). For the brush, $Z_j c_j$ in Eqs. (4) and (6) can be replaced by $\alpha\phi_b/v_m$ with ϕ_b the brush volume fraction and v_m the volume of a monomer. For the ionizable monomers of the brush (each of which carries one ionizable group), the related electrostatic plus chemical contribution to the potential μ is not zy (which it would be for a monomer of a fixed charge), but is

$$\mu^{el+chem} = \ln(1-\alpha). \tag{8}$$

For the protein it is possible to consider each of the six types of ionizable residues individually (glutamic acid, aspartic acid, and tyrosine are anionic; arginine, histidine, and lysine are cationic) as, for instance, done in Ref. [25]. However, following Ref. [5] we use a simplified approach here by considering a fixed positive charge q_f and a single type of ionizable anionic, q_-, and cationic q_+, monomer, which results for the total protein charge Z_p in

$$Z_p = q_f - q_-\alpha_- + q_+\alpha_+. \tag{9}$$

The ionization degrees α_- and α_+ follow from Eq. (7) with $z_+=1$ and $z_-=-1$. For BSA and a pH not too far from the isoelectric point pI, this simplification remains very close to a full model based on all amino acid residues [5]. The contribution $\mu^{el+chem}$ to the potential of the entire protein molecule is, in a mean-field theory, then given by [5]

$$\mu^{el+chem} = q_f y + \sum_i q_i \ln(1-\alpha_i), \tag{10}$$

with the summation running over the two types of ionizable groups. Interestingly, Eq. (10) predicts a maximum in $\mu^{el+chem}$ as a function of the local electrostatic potential y at the point where the molecule becomes uncharged. Indeed, differentiating Eq. (10) with respect to y results in

$$\frac{\partial\mu^{el+chem}}{\partial y} = q_f + \sum_i q_i z_i \frac{1}{1 + 10^{z_i(p\mathrm{H}-p\mathrm{K}_i)}e^{z_i y}} = Z_p, \tag{11}$$

a result to which we will return further on.

D. Ideal entropy term

For the protein molecules (and the small ions) we include an ideal entropy term (per particle) of

$$\mu^{ideal} = \ln\phi_i, \tag{12}$$

but leave out this term for the brush polyions, just as in traditional mean-field brush models that are based on the Flory-Huggins approach.

E. Hard-sphere, excess, or volume contribution to the chemical potential

To describe the excess contribution to the potential, we assume from this point onward that all entities are spherical; thus, their volume v_i relates to their size σ_i according to $v_i = \pi/6\sigma_i^3$. This is straightforward for ions and the (assumed spherical) globular protein molecules, but what about the polyelectrolyte chains of the brush? Our suggestion is to replace in the description of the excess function the linear chain by a certain number of spherical "beads." We then have two degrees of freedom: the size of these beads and the number of them per chain. To obtain values for these two parameters, we will use the following two constraints. The first constraint is to assume that the volume of the equivalent "string of beads" is the same as that of the original, cylindrical, chain. Second, we will assume that the beads are just touching each other. These two constraints result in a diameter of the spherical, hypothetical, beads, σ_{bead}, of $\sqrt{3/2} \sim 1.225$ times the original chain cylinder diameter σ_{cyl}.

To describe the excess function in a multicomponent mixture of spheres of different sizes, we use the BMCSL excess function [18,19], according to which the chemical potential of component i is given by [26,31]

$$\begin{aligned}\mu_i^{ex} = &-\left(1 + \frac{2\xi_2^3\sigma_i^3}{\phi^3} - \frac{3\xi_2^2\sigma_i^2}{\phi^2}\right)\ln(1-\phi) \\ &+ \frac{3\xi_2\sigma_i + 3\xi_1\sigma_i^2 + \xi_0\sigma_i^3}{1-\phi} + \frac{3\xi_2\sigma_i^2}{(1-\phi)^2}\left(\frac{\xi_2}{\phi} + \xi_1\sigma_i\right) \\ &- \xi_2^3\sigma_i^3\frac{\phi^2 - 5\phi + 2}{\phi^2(1-\phi)^3},\end{aligned} \tag{13}$$

where the ξ_α's are given by

$$\xi_\alpha = \frac{\pi}{6}\sum_i \frac{\phi_i}{v_i}\sigma_i^\alpha \tag{14}$$

and ϕ is the total volume fraction of all particles. For monodisperse systems, the classical Carnahan-Starling expression is retrieved [5,26,32,33],

$$\mu_i^{CS} = \frac{\phi(8 - 9\phi + 3\phi^2)}{(1-\phi)^3}. \tag{15}$$

In case the monovalent small ions are assumed to be infinitely small, a quite drastic simplification is possible. In this case we leave out the ions from the summations for ξ_α and add to μ^{ex} of the different other species an "ion pressure" contribution [5,24–27]

$$\mu_i^{\text{ion pressure}} = 2v_i c_\infty(\cosh y - 1), \tag{16}$$

while the chemical potential of the small ions only has a correction due to the volume ϕ, excluded to it, resulting in the "$1-\phi$" term in the Poisson equation (6).

F. Hydrophobic interactions

A final contribution to the chemical potential is an attraction of nonelectrostatic origin—e.g., due to hydrophobic forces. In line with van der Waals and Flory-Huggins theory, we describe this contribution, for component i, by

$$\mu_i^{hydr} = -v_i \sum_{j\ incl\ i} \chi_{ij}\phi_j, \tag{17}$$

where χ is defined positive when the i-j pair attracts. Note that self-interactions are also considered here and therefore interactions with the solvent are left out. When all χ parameters are the same, Eq. (17) simplifies to

$$\mu_i^{hydr} = -v_i\chi\phi. \tag{18}$$

G. Summary of contributions to the potential

In summary, the potential per protein molecule has the following contributions: (i) the ideal contribution, $\ln\phi_i$ of Eq. (12); (ii) the electrostatic plus chemical contribution of Eq. (10); (iii) an excess term given by Eq. (13); and (iv) a hydrophobic contribution using Eq. (17).

For the brush, the different contributions to the potential (defined per nm of chain length) are (i) the stretching term of Eq. (2) (with k in nm); (ii) the electrical plus chemical contribution of Eq. (8), multiplied by λ, the number of monomers per nm chain; (iii) an excess term given *per bead* by Eq. (13), which must therefore be divided by σ_{bead} to obtain the contribution per nm chain length; and (iv) a hydrophobic contribution due to Eq. (17).

When ion volume is neglected, we use Eq. (6) instead of Eq. (4), leave the ions out of the summation for ξ_α, and add to the potential of brush segments and protein an ion pressure term, given by Eq. (16).

H. Comparison of BMCSL with Flory-Huggins theory

In the absence of other species, the excess, or volume, potential of a brush segment is given by Eq. (15), which can be expanded in

$$\mu_i^{ex} = \frac{1}{\sigma_{bead}}(8\phi + 15\phi^2 + \cdots), \tag{19}$$

to which we can add a hydrophobic contribution according to Eq. (18), after which we have two adjustable parameters, the second and third virial coefficients, in complete similarity to the usual approach based on expansion of the logarithmic term in Flory-Huggins theory. For such a one-component brush the present approach clearly does not make a difference; it is only when we start considering adsorption in the brush of (globular) species of sizes quite different from the typical brush segment that the use of Eqs. (13) and (14) becomes useful.

I. Mass conservation

Conservation of brush segment volume results in

$$\frac{\pi}{4}\sigma_{cyl}^2 L\sigma^* R^2 = \int_R^D \phi_b r^2 \mathrm{d}r, \tag{20}$$

where σ^* is the grafting density and $4\pi\sigma^* R^2$ the total number of chains on each spherical carrier particle. The right-hand side integrates the polyion volume over the brush coordinate.

III. RESULTS AND DISCUSSION

A. Boundary conditions

To solve Poisson's equation, Eq. (4) or Eq. (6), we assume that the carrier particle is uncharged, and thus $\mathrm{d}y/\mathrm{d}r=0$ at $r=R$, while at the edge of the brush, $r=D$, both the potential y and its derivative $\mathrm{d}y/\mathrm{d}r$ are continuous. Outside the brush the potential goes to zero in a few Debye lengths, described by Eq. (4) or Eq. (6) with the concentration of brush segments set to zero. At the brush edge, the brush density becomes zero ($\phi=0$).

Instead of Poisson's equation, we also solved the brush model while assuming local charge electroneutrality—that is, by setting the left-hand side of Eq. (4) or Eq. (6) to zero (namely, in Fig. 4 and one curve in Fig. 6). For the larger part of the brush this simplication makes no difference; indeed, the brush is charge neutral there. Correspondingly, the predicted adsorbed amount of protein is the same in both methods. The only, quite interesting, difference is in the brush profile at the edge of the brush; see Fig. 1 for a polyacrylic acid brush in the absence of protein (pH 10, 10 mM salt). Here, the curve "EN" is based on assuming local charge neutrality at each distance x from the surface, whereas "Poisson" denotes a calculation based on the full Poisson equation. In the first case, the brush density gradually goes down to zero, as expected. However, using the full Poisson equation, we observe that the predicted density profile sharply drops at the very tip of the brush. We find that this sharp drop becomes the more important the more higher-order corrections to the parabolic profile for the conformational term are implemented in Eq. (2). We believe this phenomenon is due to charge separation at the edge of the brush: here local charge neutrality is not required because the diffuse layer outside the brush is so close by and the system can gain conformational energy by retracting the free chain ends in that region slightly, without a concomitant electrostatic energy penalty. The higher the number of terms that are introduced in Eq. (2), and so the more the brush deviates from classical Gaussian behavior, the more energy is released upon a slight retraction of the final part of the brush.

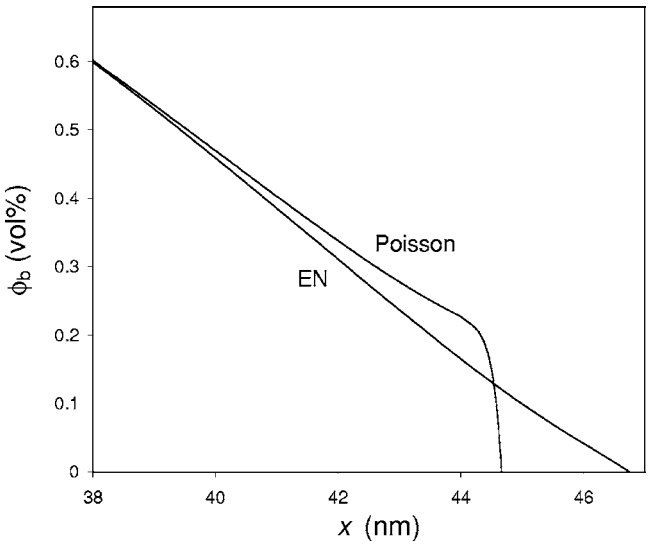

FIG. 1. Density profile of non-Gaussian polyacrylic acid brush using local charge neutrality ("EN") or the full Poisson equation (SS40, pH=10, c_∞=10 mM).

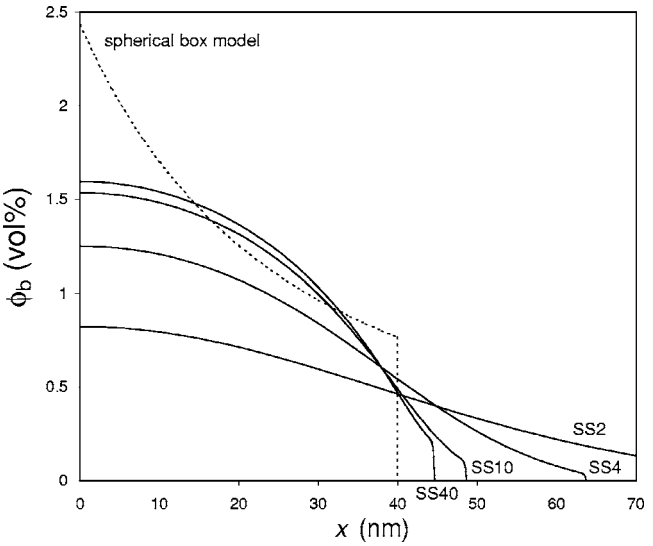

FIG. 2. Spherical polyelectrolyte brush. Brush density in vol. % as function of distance from the grafting core particle, x (pH=10, n_∞=10 mM). The dashed line is box model of Ref. [5], and solid lines are based on the strong-stretching approximation. "SS2" is based on a purely parabolic profile for the stretching contribution to the chemical potential; SS4, SS10, and SS40 denote higher-order corrections.

B. Parameter settings

For the globular BSA molecule we use q_f=73 for the number of positive fixed charges and q_-=100 and q_+=16 for the number of anionic and cationic ionizable groups [5]. For the former, we use $p\mathrm{K}_-$=4.2 (aspartic acid, glutamic acid) and $p\mathrm{K}_+$=6.9 (histidine) for the latter, which results in an isoelectric point pI of 5.1, in agreement with experiment. We use a volume of v_p=100 nm^3, thus a size (for the equivalent sphere) of σ_p=5.76 nm. In all cases the protein concentration in solution is 2 mg/ml, corresponding to ϕ_∞=0.18 vol. %.

For the polyacrylic acid brush (anionic, z=−1) we assume pK=4.2 (just as for aspartic and glutamic acid) and use a Kuhn length k of 1 nm, thus 4 times that of the carboxylic monomeric unit of $a=1/\lambda$=0.25 nm [5]. The chain has a contour length of L=50 nm and a cylindrical diameter of σ_{cyl}=0.5 nm; the chemical potential is calculated per segment which is defined as a 1-nm stretch of chain, thus of volume v_b=0.196 nm^3 (monomer volume v_m=0.049 nm^3). The bead size and volume, to be used in Eqs. (13) and (14), are given by σ_{bead}=0.612 nm and v_{bead}=0.12 nm^3. The carrier particle on which the chains are grafted has a radius of R=50 nm, a mass density of 1.06 gr/ml, and thus a mass of 0.56 fg. The grafting density is σ^*=0.1 nm^{-2}.

C. Non-Gaussian chains

We compare the strong-stretching brush model with the spherical box model [5] in Fig. 2 for an assumed parabolic dependence of the conformational contribution to the potential, μ^{conf}, as function of distance x from the grafting surface (SS2), as well as with higher-order terms incorporated, denoted by SS4, SS10, and SS40, the number corresponding to the maximum power considered in the series of Eq. (2).

In this case, using the classical parabolic profile for μ^{conf} (SS2), we find a brush thickness almost twice the contour length of L=50 nm, and higher-order corrections are required to bring x/L to below unity. Unfortunately, the convergence of Eq. (2) is quite slow and we need a large number of such terms (in this case up to SS30 at least). Comparing with the box model we see a quite different brush density profile with, as expected, a more gradual decline of brush density predicted in case of the strong-stretching approach.

D. Electrostatic barrier to protein transfer across outer edge of a polyelectrolyte brush

Protein adsorption in a brush that is of opposite charge sign is not difficult to understand. However, the possibility that protein adsorbs in a brush of a like charge sign is more counterintuitive, certainly when nonelectrostatic attractions are neglected. Indeed, for a particle that has a fixed charge this is impossible (in the 1D mean-field model of this paper), but for protein molecules near their isoelectric point it is well possible that the charge of the molecule is reversed upon entry into the brush. The question is, does this lead to an attractive term?

In Fig. 3 we plot the electrochemical potential change when a particle moves from the solution phase where the electrostatic potential y is zero into a polyanion brush where $y<0$. For a particle of a fixed charge Z, $\Delta\mu^{el}$ is given by Zy and with both $y<0$ and $Z<0$ the particle feels an increasing repelling force closer to, and deeper in, a negatively charged brush (dashed line).

For an amphoteric particle, however, the situation is different. Based on Eqs. (9) and (10) we plot $\Delta\mu^{el+chem}$ as a function of y and pH for the protein BSA. In the right-hand part of the graph we see that when BSA moves toward the brush, with y gradually decreasing, $\Delta\mu^{el+chem}$ initially increases, representing a barrier to protein transfer. However,

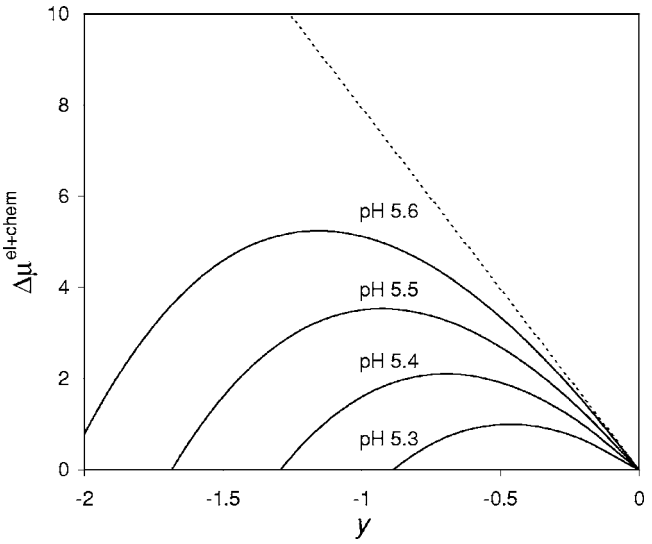

FIG. 3. Electrochemical potential of the amphoteric protein molecule as a function of electrostatic potential y and pH (solid lines). For a particle of a fixed negative charge, μ monotonically increases with decreasing y (dashed line).

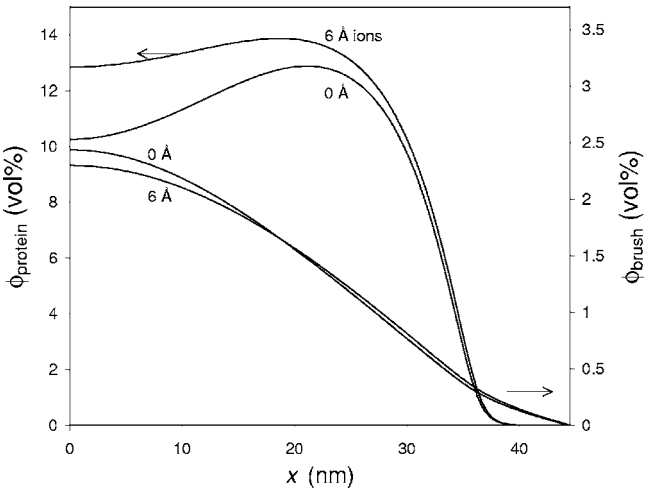

FIG. 4. Influence of (hydrated) ion size (in Å) on protein and brush density profiles (c_∞=10 mM, pH 5.4, pI 5.1, χ=0). x is the distance from the core particle, and ϕ is the volume fraction of protein and brush segments.

going further to the left and arriving below a critical y value [which corresponds to the molecule being exactly uncharged; see Eq. (11)], $\Delta\mu^{el+chem}$ starts to decrease again with the molecule now positively charged. Beyond that point (below that y value in the brush) the protein molecule experiences a driving force towards more negative regions (deeper into a poyanion brush). For each pH value there is a (second) critical value for the electrostatic potential in the brush, y^*, below which $\Delta\mu^{el+chem}$ becomes negative, and a net driving force develops for protein to transfer from the solution phase into the brush. With increasing pH, y^* decreases, and it becomes progressively more difficult to realize a negative value for $\Delta\mu^{el+chem}$. Thus, only when pH is not too far above pI is y^* still small and is it possible for protein to be adsorbed into the brush (which requires $\Delta\mu^{el+chem}<0$).

E. Effect of ion volume

Before going into the effect of pH and ionic strength on the adsorption profiles, let us briefly compare theoretical predictions using a zero ion volume ("0 Å" in Fig. 4) and a value for the ion size of 6 Å, which is typical for an ion together with its hydration shell. It is well accepted that for monovalent salt at a not too high ionic strength the diffuse layer of ions next to a charged interface can be accurately described using the Poisson-Boltzmann equation, which assumes that the ions are point charges (thus, of zero volume). Indeed, making such a calculation for c_∞=10 mM, we find that even at a quite high surface charge of 50 mC/m^2 (0.3 charges per nm^2) the deviation is negligible ($\sim$2%, with the surface potential $\sim$100 mV).

Interestingly, for the same ionic strength, we see in Fig. 4 that in a brush with coadsorbed protein molecules, the size of

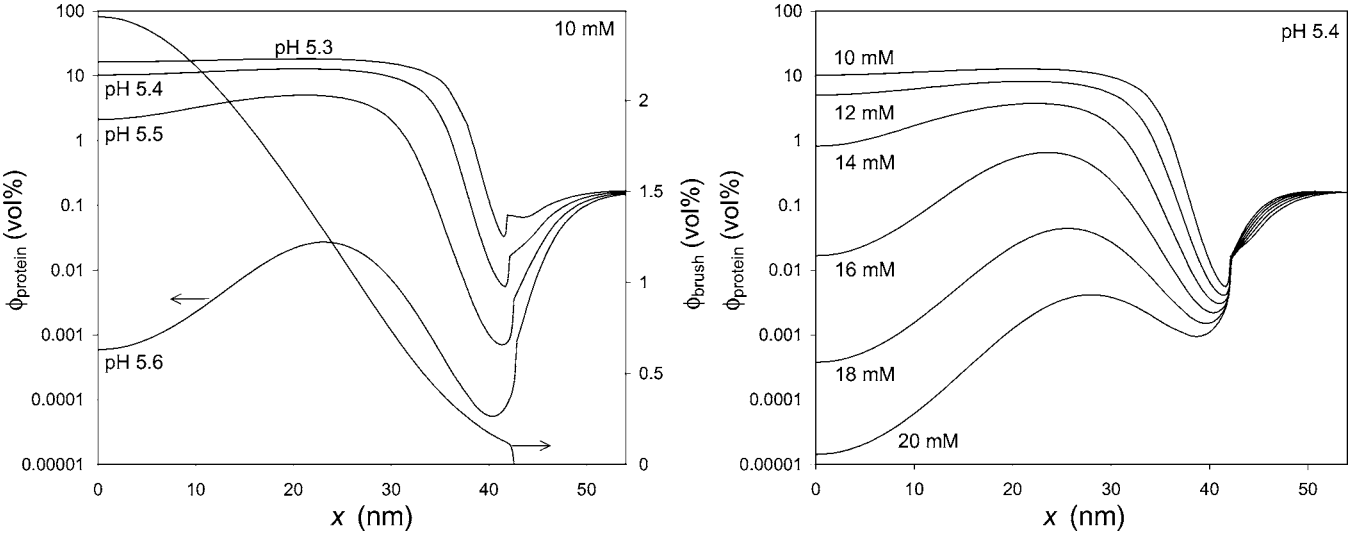

FIG. 5. Protein adsorption in a spherical polyanion brush as function of ionic strength and pH. Conditions of Fig. 4.

the ions can make a significant difference to the density profiles, especially of the coadsorbed protein, the concentration of which increases upon an increase in the size of the ions. This is due to the fact that with increasing ion size, its incorporation in the brush becomes more "expensive" and charge compensation of the polyion chains using the protein molecules instead of the small counterions becomes slightly more favorable, leading to an enhanced protein adsorption.

F. Protein adsorption in a polyelectrolyte brush

In Fig. 5 we present density profiles of adsorbed protein as function of *p*H and ionic strength (the brush profile is rather invariant over the parameter range, and thus only one curve is shown; ion size 0 Å, $\chi=0$). Significant protein adsorption is predicted at $p\mathrm{H} > p\mathrm{I}$ (at *p*H 5.3 up to 18 vol. %), though the protein molecules in solution have the same charge sign as the polyanion brush. At low *p*H (but $>p$I) the protein density profile $\phi_p(x)$ in the brush is quite flat, with a steep decrease of ϕ_p near the edge of the brush where y is most unfavorable (corresponding to the maximum in $\mu^{el+chem}$ of Fig. 3). Outside the brush, ϕ_p slowly increases again, toward the bulk value.

Indeed, just outside the brush, in all cases the protein concentration is lower than the bulk value; thus, the nonadsorbed molecules are effectively repelled from the brush. Interestingly, it is due to this repulsion that a stable, bidisperse, colloidal dispersion can be obtained consisting of the (protein-filled) spherical brush particles, and the nonadsorbed protein, as is experimentally observed [1,4]. This is not possible for a *p*H below *p*I, in which case protein is positively charged and the mixture coagulates.

Going from *p*H 5.3 to higher *p*H values, we find that the density profile of protein in the brush becomes more nonmonotonic, with ϕ_p deep in the brush (near $x=0$) becoming much lower than its value halfway in the brush [for *p*H 5.5 $\phi_p(x=0)=2.1$ vol. % vs $\phi_p(x=21\ \mathrm{nm})=5$ vol. %] because volume interactions of protein molecules with the brush segments come into play (with ϕ_{brush} being highest at $x=0$). The protein concentration near the edge of the brush decreases further, even to values as low as 0.5% of the bulk value (at *p*H 5.5). At even higher *p*H we can no longer speak of adsorption of protein: the concentration of protein near and in the brush is below the bulk value.

When we go to more unfavorable conditions for protein adsorption either by increasing *p*H or by increasing the ionic strength, we see interesting differences in how the height of the energy barrier to protein transfer at the edge of the brush develops (note that a lower protein concentration corresponds to a higher-energy barrier). Comparing, for instance, the curve for *p*H 5.6 in Fig. 5(a), with the curve for 20 mM ionic strength in Fig. 5(b), we see for a *p*H increase a much sharper and deeper minimum in protein concentration developing at the edge of the brush, corresponding to a higher "barrier" to protein transfer across this region. Interestingly, this behavior corresponds to an observed difference in the reversibility of protein adsorption and desorption as function of *p*H and ionic strength [39]—namely, that after protein adsorption, upon an increase of ionic strength protein is quite readily released [1,2], but much less so upon an increase of *p*H.

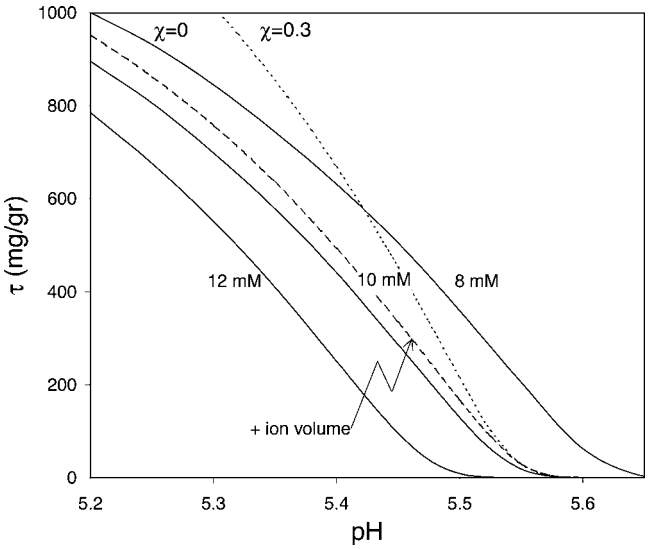

FIG. 6. Adsorbed amount of protein in a spherical brush particle, as function of *p*H, ionic strength, attraction parameter χ, and ion size (0 Å, except for the curve "+ion volume").

Finally, Fig. 6 shows the protein adsorbed amount τ (in mg per g of carrier particle) as a function of *p*H, ionic strength, attraction strength, χ, and ion size. When we include a nonelectrostatic attraction it is by using Eq. (18) in which brush-brush, protein-protein, and protein-brush interactions are described alike, using the same χ value. Like in the box model calculation of Ref. [5] we find that the adsorbed amount increases rapidly in a quite small *p*H or ionic strength window. The transition from low to high adsorbed amount, τ, is slightly accelerated when we add ion size effects, and quite significantly so when we include a nonelectrostatic attraction term. Clearly, the protein adsorption isotherms of Refs. [1,2] cannot yet be quantitatively reproduced.

IV. CONCLUSIONS

To describe the adsorption of globular protein in a polymer structure, we have used the Boublik-Mansoori-Carnahan-Starling-Leland excess function for multicomponent mixtures of spheres. We describe the polymer chain as a string of touching beads and use the strong-stretching approach of the self-consistent-field equation to describe the conformational contribution to the potential, including higher-order corrections to the parabolic profile.

Results are presented for the adsorption of ionizable globular protein into a spherical polyelectrolyte brush. In line with earlier box model calculations we again find that protein adsorption in a polyelectrolyte brush of the same charge sign is indeed possible as long as *p*H is still close to the isoelectric point and the ionic strength is sufficiently low, due to the fact that the protein molecule is amphoteric—that is, is able to reverse its charge upon entering the brush. A minimum in protein concentration is predicted at the edge of the brush,

possibly representing a kind of "barrier" for protein to desorb from the brush.

ACKNOWLEDGMENTS

This work was financially supported by NWO, Netherlands Organisation for Scientific Research. Discussions with Matthias Ballauff, Alexander Wittemann (Bayreuth), and Hans-Hennig von Grünberg (Graz) are kindly acknowledged.

APPENDIX: FREE ENERGY ANALYSIS

In this appendix we analyze the free energy particle change upon protein adsorption in a polyelectrolyte brush. We base the calculation on the conditions of Fig. 4 for a zero ion size (pH 5.4, $c_\infty = 10$ mM, $\chi = 0$). For this case, 2232 protein molecules adsorb in the brush, and with a total of 3142 brush chains, we thus have 0.71 adsorbed protein molecules per chain. We use the same brush density profile $\phi_b(x)$ and brush height H for both an empty and a protein-filled brush. Thus, we neglect the fact that the brush density profile changes (slightly) when protein adsorbs. Furthermore, we assume local electroneutrality at each location x in the brush and, therefore, can neglect the electric field energy [25,36–38]. What remains in the free energy balance is entropy, excess (volume) contributions, and chemical terms, related to proton binding to the chareged polymer groups.

The grand-canonical free energy per carrier particle is obtained from a volume integration over the system (brush) of the grand-canonical free energy density, ω. This term combines the free energy density f with the adsorption of ions and protein molecules from the (infinitely large) reservoir

$$\omega = f - \sum_i c_i \mu_{i,\infty}, \tag{A1}$$

where c_i is the local concentration of either ions or protein molecules in the brush and $\mu_{i,\infty}$ their potential in the reservoir. We incorporate the ideal, entropic, part of μ directly in f [see Eq. (A3)]. The free energy density f has the following five contributions:

$$f = f^{\text{protein entropy}} + f^{\text{ex}} + f^{\text{ion entropy}} + f^{\text{chem protein}} + f^{\text{chem brush}}. \tag{A2}$$

First of all, the ideal, entropy, terms, for both protein and the two types of ions, is given by

$$f^{\text{entropy}} = \sum_i \left(c_i \ln \frac{c_i}{c_{i,\infty}} - c_i + c_{i,\infty} \right). \tag{A3}$$

For the volumeless ions, Eq. (A3) can be simplified by inserting $c_i = c_{i,\infty}(1-\phi)e^{-z_i y}$.

The excess term is given by [34]

$$f^{\text{ex}} = \frac{6}{\pi}\left[-\xi_0 \ln(1-\phi) + 3\frac{\xi_1\xi_2}{1-\phi} + \xi_2^3 \frac{\phi + (1-\phi)^2 \ln(1-\phi)}{\phi^2(1-\phi)^2} \right], \tag{A4}$$

with ϕ the total volume of protein and chains and where we must include the small ions in the local number density, ξ_0.

The chemical contributions for the ionizable monomers are given by [24,35]

$$f^{\text{chem protein}} = c_p\{q_-[\ln(1-\alpha_-) + \alpha_- y] + q_+[\ln(1-\alpha_+) - \alpha_+ y]\}, \tag{A5}$$

$$f^{\text{chem brush}} = c_m\{\ln(1-\alpha) + \alpha y\}, \tag{A6}$$

with c_p and c_m the number concentration of protein molecules and brush monomers, respectively; q_+ and q_- are the numbers of anionic and cationic amino acids per protein molecule.

The chemical contribution can be derived as follows. When a certain number of protons has desorbed from an anionic material the chemical energy released (per site) is given by (Ref. [35], p. 439)

$$f^C = \alpha \ln \alpha + (1-\alpha)\ln(1-\alpha) + \alpha \Delta\mu_{des} + \alpha \ln c_{H,\infty}, \tag{A7}$$

where α is the ionization degree (fraction of sites from which a proton has desorbed), $\Delta\mu_{des}$ the (standard-state) proton desorption energy, and $c_{H,\infty}$ the proton concentration in the reservoir. $\Delta\mu_{des}$ relates to the intrinsic pK of the material according to $\Delta\mu_{des} = \ln 10 \cdot p\text{K}$ while $\ln c_{H,\infty} = -\ln 10 \cdot p\text{H}$. Together with Eq. (7) ($z=-1$), we can rewrite Eq. (A7) to obtain [24]

$$f^C = \ln(1-\alpha) - z\alpha y. \tag{A8}$$

Multiplying by the local monomer concentration results in Eq. (A6). Equation (A5) is slightly more complicated because we sum over both cationic ($z=1$) and anionic amino acid residues.

The potential of the protein molecule in solution, $\mu_{p,\infty}$, has an ideal contribution given by Eq. (12) [which is already included in Eq. (A3)] and contributions from Eqs. (10), (15), and (16). These three contributions must be redistributed into an excess term

$$\mu_{p,\infty}^{ex} = \frac{\phi(8 - 9\phi + 3\phi^2)}{(1-\phi)^3} + 2c_\infty v_p(\cosh y - 1), \tag{A9}$$

an ion entropy term

$$\mu_{p,\infty}^{\text{ion entropy}} = Z_\infty y_\infty, \tag{A10}$$

and a chemical term

$$\mu_{p,\infty}^{\text{chem protein}} = q_-[\ln(1-\alpha_{-,\infty}) + \alpha_{-,\infty} y_\infty] + q_+[\ln(1-\alpha_{+,\infty}) - \alpha_{+,\infty} y_\infty], \tag{A11}$$

where Z_∞ is the total protein charge, given by Eq. (9). These three $\mu_{p,\infty}$ terms are each multiplied by c_p and subtracted from the corresponding four terms in f to obtain ω which can be integrated over the total brush volume to obtain the grand-canonical free energy per carrier particle.

The total free energy change upon protein adsorption is calculated as $\Delta F^{\text{tot}} = -4.4$ kT per chain, which is negative (as it should be for a spontaneous process). But how does ΔF^{tot} break down in the different contributions? Let us first discuss the positive contributions—i.e., those that must be overcome

by other forces. First of all there is the ideal entropy of the protein molecules themselves, which is $\Delta F^{\text{protein entropy}} = +2.2$ kT. Next, we have volume interactions between the adsorbed protein molecules and the brush chains, amounting to $\Delta F^{\text{ex}} = +20.3$ kT. The largest contribution, however, is the cost of charge reversing the protein molecules, which amounts to $\Delta F^{\text{chem protein}} = +57.4$ kT per chain (+84.4 kT per protein molecule). The total sums up to +84.3 kT per chain.

The two driving forces, which together must generate an 84.3 kT energy release, are ion entropy and the chemical contribution for the brush. Ion entropy ("ion release") turns out to be the largest contributor, $\Delta F^{\text{ion entropy}} = -59.9$ kT. However, the increase in brush ionization is not to be neglected, $\Delta F^{\text{chem brush}} = -24.4$ kT, and thus constitutes 30% of the total driving force.

In conclusion, ion release (in a one-dimensional model only possible after the protein molecule has charge reversed) and an increase in ionization of the brush segments are the two driving forces for protein adsorption in a like-charged polyelectrolyte brush.

[1] A. Wittemann, B. Haupt, and M. Ballauff, Phys. Chem. Chem. Phys. **5**, 1671 (2003).
[2] A. Wittemann, B. Haupt, R. Merkle, and M. Ballauff, Macromol. Symp. **191**, 81 (2003).
[3] S. Rosenfeldt, A. Wittemann, M. Ballauff, E. Breininger, J. Bolze, and N. Dingenouts, Phys. Rev. E **70**, 061403 (2004).
[4] A. Wittemann and M. Ballauff, Anal. Chem. **76**, 2813 (2004).
[5] P. M. Biesheuvel and A. Wittemann, J. Phys. Chem. B **109**, 4209 (2005).
[6] A. N. Semenov, Sov. Phys. JETP **61**, 733 (1985).
[7] A. M. Skvortsov, I. V. Pavlushkov, A. A. Gorbunov, E. B. Zhulina, O. V. Borisov, and V. A. Pryamitsyn, Polym. Sci. U.S.S.R. **30**, 1706 (1988).
[8] E. B. Zhulina, V. A. Pryamitsyn, and O. V. Borisov, Polym. Sci. U.S.S.R. **31**, 205 (1989).
[9] S. T. Milner, T. A. Witten, and M. E. Cates, Macromolecules **21**, 2610 (1988).
[10] S. J. Miklavic and S. Marçelja, J. Phys. Chem. **92**, 618 (1988).
[11] S. T. Milner, T. A. Witten, and M. E. Cates, Macromolecules **22**, 853 (1989).
[12] D. F. K. Shim and M. E. Cates, J. Phys. (France) **50**, 3535 (1989).
[13] S. T. Milner, Science **251**, 905 (1991).
[14] S. Misra and S. Varanasi, J. Chem. Phys. **95**, 2183 (1991).
[15] Yu. V. Lyatskaya, F. A. M. Leermakers, G. J. Fleer, E. B. Zhulina, and T. M. Birshtein, Macromolecules **28**, 3562 (1995).
[16] V. M. Amoskov and V. A. Pryamitsyn, J. Chem. Soc., Faraday Trans. **90**, 889 (1994).
[17] V. M. Amoskov and V. A. Pryamitsyn, Macromol. Theory Simul. **12**, 223 (2003).
[18] T. Boublik, J. Chem. Phys. **53**, 471 (1970).
[19] G. A. Mansoori, N. F. Carnahan, K. E. Starling, and T. W. Leland, J. Chem. Phys. **54**, 1523 (1971).
[20] A. Galindo, P. J. Whitehead, G. Jackson, and A. N. Burgess, J. Phys. Chem. **100**, 6781 (1996).
[21] C. Simmons, S. E. Webber, and E. B. Zhulina, Macromolecules **34**, 5053 (2001).
[22] Y. Moskovitz and S. Srebnik, Biophys. J. **89**, 22 (2005).
[23] F. Fang, J. Satulovsky, and I. Szleifer, Biophys. J. **89**, 1516 (2005).
[24] P. M. Biesheuvel, Eur. Phys. J. E **16**, 353 (2005).
[25] P. M. Biesheuvel, M. van der Veen, and W. Norde, J. Phys. Chem. B **109**, 4172 (2005).
[26] P. M. Biesheuvel and J. Lyklema, J. Phys.: Condens. Matter **17**, 6337 (2005).
[27] T. Biben and J.-P. Hansen, J. Phys.: Condens. Matter **6**, A345 (1994).
[28] D. Y. C. Chan and D. J. Mitchell, J. Colloid Interface Sci. **95**, 193 (1983).
[29] O. V. Borisov, A. B. Boulakh, and E. B. Zhulina, Eur. Phys. J. E **12**, 543 (2003).
[30] P. M. Biesheuvel, J. Phys.: Condens. Matter **16**, L499 (2004).
[31] L. Lue, N. Zoeller, and D. Blankschtein, Langmuir **15**, 3726 (1999).
[32] N. F. Carnahan and K. E. Starling, J. Chem. Phys. **51**, 635 (1969).
[33] G. A. Vliegenthart and H. N. W. Lekkerkerker, J. Chem. Phys. **111**, 4153 (1999).
[34] S. M. Oversteegen and R. Roth, J. Chem. Phys. **122**, 214502 (2005).
[35] Th. A. J. Payens, Philips Res. Rep. **10**, 425 (1955).
[36] J. Th. G. Overbeek, Colloids Surf. **51**, 61 (1990).
[37] D. Harries, S. May, W. M. Gelbart, and A. Ben-Shaul, Biophys. J. **75**, 159 (1998).
[38] M. Manciu and E. Ruckenstein, Langmuir **19**, 1114 (2003).
[39] A. Wittemann (private communication).